

# Ab-initio nanoplasmonics: atoms matter

Pu Zhang,<sup>1</sup> Johannes Feist,<sup>1</sup> Angel Rubio,<sup>2,3</sup> Pablo García-González,<sup>1,3,\*</sup> and F. J. García-Vidal<sup>1,†</sup>

<sup>1</sup>*Departamento de Física Teórica de la Materia Condensada and Condensed Matter Physics Center (IFIMAC),  
Universidad Autónoma de Madrid, E-28049 Cantoblanco, Madrid, Spain*

<sup>2</sup>*Nano-Bio Spectroscopy group, Universidad del País Vasco UPV/EHU,*

*CFM CSIC-UPV/EHU-MPC and DIPC, Avenida de Tolosa 72, E-20018 Donostia, Spain*

<sup>3</sup>*ETSF Scientific Development Centre, E-20018 Donostia, Spain*

(Dated: December 6, 2024)

We present an ab-initio study of the hybridization of localized surface plasmons in a metal nanoparticle dimer. The atomic structure, which is often neglected in theoretical studies of quantum nanoplasmonics, has a strong impact on the optical absorption properties when sub-nanometric gaps between the nanoparticles are considered. We demonstrate that this influences the hybridization of optical resonances of the dimer, and leads to significantly smaller electric field enhancements as compared to the standard jellium model. In addition we show that the corrugation of the metal surface at a microscopic scale becomes as important as other well-known quantum corrections to the plasmonic response, implying that the atomic structure has to be taken into account to obtain quantitative predictions for realistic nanoplasmonic devices.

PACS numbers: 42.25.Bs, 36.40.Gk, 78.67.Bf, 73.20.Mf

There is a growing interest in the development and implementation of nanoplasmonic devices such as nanosensors [1, 2], nanophotonic lasers [3–5], optoelectronic [6, 7] and light-harvesting [8, 9] structures, and nanoantennas [10, 11]. Therefore, it is essential to have theoretical techniques with sufficient predictive value for understanding the physical processes of light-matter interaction at the nanoscale. In this regime, the standard analysis of the plasmonic response to external electromagnetic (EM) fields using the classical macroscopic Maxwell equations must be undertaken with caution. Indeed, genuine quantum effects such as the nonlocal nature of the electron-density response, the inhomogeneity of the conduction-electron density, or the possibility of charge transfer by tunneling have to be considered [12]. These effects can be incorporated into Maxwell equations in an approximate manner using, e.g., nonlocal dielectric functions [13–19] or the *ad-hoc* inclusion of “virtual” dielectric materials [20–22]. While these semi-classical approximations have been successfully applied in many cases, they never achieve the precision provided by first-principle calculations.

A number of recent publications [20, 23–27] have treated the electronic response of plasmonic structures using state-of-the-art time-dependent density functional theory (TDDFT) [28, 29]. However, the ionic structure is typically neglected and replaced by a homogeneous jellium background or by an unstructured effective potential. Although this approximation is sometimes justified by the collective nature of plasmon excitations [30, 31], the charge oscillations associated with a localized surface plasmon (LSP) are mainly concentrated on the metal-vacuum interface. One may thus expect that the ionic structure in this region will have quantitative and even qualitative impact. Therefore, there is a need to address the influence of the atomic configuration in the plasmonic response at the nanoscale.

In this Letter, we present ab-initio calculations including the atomic structure, in accordance with the current paradigm in computational condensed matter physics [32] and physical chemistry [33]. We study one of the canonical cases in nanoplasmonics: the hybridization of LSPs in a metallic-cluster dimer. This structure has received widespread attention from a theoretical perspective in the last years [23, 24, 34, 35], and has recently been experimentally realized in nanodevices with sub-nanometric gaps [36, 37]. Furthermore, this is one of the prototypic plasmonic systems where quantum effects are relevant [38]. First, the coexistence of different natural length scales requires taking into account the non-locality of the response to EM fields. Second, the hybridization will depend very sensitively on the spacing between the effective surfaces of the clusters, which is determined by the amount of electron-density spill-out at the metal-vacuum interfaces [25, 39]. Finally, if the distance between the clusters is small enough, incident EM radiation can establish an alternating tunnel current between the two clusters, which greatly affects the electric field enhancement (EFE) in the interstitial region [23, 24].

Specifically, we analyze the optical response of a sodium nanocluster dimer, although the conclusions can be extended to any other metallic dimer, e.g. gold or silver. Only the  $3s$  conduction electrons are explicitly included in the calculation by using standard norm-conserving Troullier-Martins pseudopotentials [40]. Each cluster consists of  $N = 331$  atoms which are arranged symmetrically around a central atom on the BCC Na lattice (see the inset of [fig. 1](#)). The corresponding lattice constant is set to the experimental value of bulk Na ( $a = 0.423$  nm). This realistic description will be compared against the jellium model, where the positive background is a homogeneous sphere of diameter  $2R = 2.88$  nm. This is a fair comparison due to the high symmetry of the arrangement of the atoms in the  $\text{Na}_{331}$

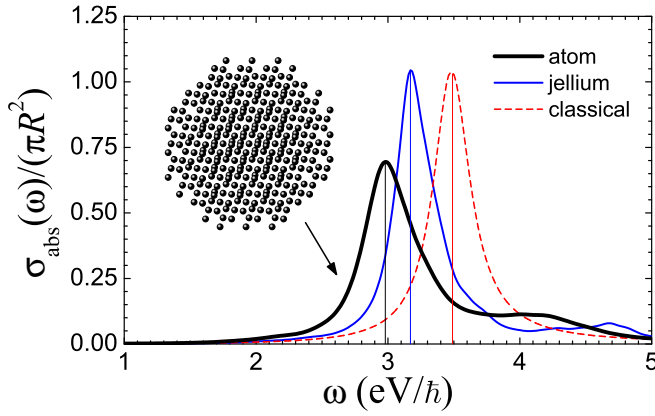


FIG. 1: (Color online). Normalized TDDFT optical absorption cross section for an isolated BCC  $\text{Na}_{331}$  cluster. Thick black line: atomistic description, thin blue line: jellium model. For completeness, the corresponding classical local-optics result (dashed red line) is included as well. The latter has been artificially broadened in order to fit the width of the main absorption peak of the jellium cluster. The main-resonance energies,  $\hbar\omega_M$ , are: 2.98 eV (atom/TDDFT), 3.17 eV (jellium/TDDFT), and 3.49 eV (classical local optics).

cluster. Furthermore, we have checked that the relaxation of the atoms in each cluster leads to a minor distortion of the BCC arrangement. The only noticeable effect is a slight overall compression, which should be reflected in the jellium model by reducing the value of  $R$  and consequently increasing the density of the jellium background. Since our aim is to analyze the impact of the atomic structure *per se*, in what follows we will work with non-relaxed structures [41]. Finally, we define the separation between the clusters as  $d = b - 2R$  for both the atomic and jellium cases, where  $b$  is the distance between the central atoms of each cluster or between the centers of the jellium spheres.

Due to the nanometric size of the system, retardation effects can be safely ignored. The optical response can thus be evaluated using TDDFT under the adiabatic local density approximation, which is appropriate for simple metals such as Na [42–44]. To solve the TDDFT equations we follow a time-propagation/real-space prescription [45] as implemented in the OCTOPUS package [46, 47]. According to this recipe, the ground-state electron system is perturbed at  $t = 0$  by a delta-kick electric field  $\mathbf{E}(\mathbf{r}, t) = (\hbar\kappa_0/e)\delta(t)\mathbf{e}_x$ , where  $e$  is the absolute value of the electron charge and  $\kappa_0$  is small enough to ensure a linear response by the electrons. As a result, the Kohn-Sham (KS) wavefunctions at  $t = 0^+$  are  $\psi_i(\mathbf{r}, 0^+) = \exp(i\kappa_0 x)\psi_i(\mathbf{r})$ , where  $\psi_i(\mathbf{r})$  are the unperturbed ground-state KS orbitals. After this initial step, the time-dependent KS equations are solved in a real-domain representation and, in particular, the induced time-dependent electron density  $\delta n(\mathbf{r}, t)$  is obtained. Its frequency representation

is thus given by

$$\delta n(\mathbf{r}, \omega) = \int_0^{T_{\max}} \delta n(\mathbf{r}, t) e^{(i\omega - \gamma)t} dt, \quad (1)$$

where  $T_{\max}$  is the total propagation time and  $\gamma = 0.10$  eV/ $\hbar$  is a damping frequency which simulates non-electronic losses. Therefore,  $(E_0 e / \hbar \kappa_0) \delta n(\mathbf{r}, \omega)$  is the complex induced electron density by a monochromatic perturbing field  $E_0 \exp(-i\omega t) \mathbf{e}_x$ . The absorption cross section is given by  $\sigma_{\text{abs}}(\omega) = (\omega / c \epsilon_0) \Im \alpha(\omega)$ , where

$$\alpha(\omega) = -\frac{e^2}{\hbar \kappa_0} \int x \delta n(\mathbf{r}, \omega) d\mathbf{r}, \quad (2)$$

is the dynamical polarizability. Well-converged results are obtained after  $2 \times 10^4$  time steps with a total propagation time  $T_{\max} \simeq 40$  fs, using a grid spacing of 0.026 nm.

Optical properties of large isolated sodium clusters have been studied extensively in a recent article by Li *et al.* in the size range  $N \leq 331$  [48]. Our results in fig. 1 are fully consistent with theirs. For an isolated cluster, the atom/TDDFT and jellium/TDDFT optical absorption spectra are qualitatively similar. However, the proper incorporation of the atomic structure is reflected in an overall red-shift of the spectrum, as well as in an increased linewidth of the main peak. As is well known, this peak corresponds to a dipole LSP or Mie resonance and, under a quantum treatment, its width is due to Landau fragmentation plus non-electronic damping processes [48, 49]. The difference between the atom/TDDFT and jellium/TDDFT predictions for the peak frequency  $\omega_M$  are practically the same as the difference between the jellium/TDDFT and the classical predictions. This indicates that the distortion of the electron density due to atomic structure plays a quantitatively similar role as the electron density spill-out, whose absence is one of the main sources of error in classical local optics.

We now analyze the optical absorption of  $\text{Na}_{331}$  dimers in the range of sub-nanometric separations ( $0.1 \leq d \leq 0.5$  nm). The results for the three prescriptions that we are considering (atom/TDDFT, jellium/TDDFT, local optics) are presented in fig. 2. Since the differences between the frequencies of the dipole LSP in the isolated cluster are reflected in the corresponding optical absorption spectra, we normalize the frequency  $\omega$  of the incident EM field to the frequency  $\omega_M$  for each prescription. The main trends in the hybridization process can be well understood in terms of classical optics [34]. This description breaks down for small separations, where charge transfer between the clusters is possible [23]. As shown in fig. 2, the jellium/TDDFT and the classical spectra agree well in the range  $d \geq 0.4$  nm, where charge transfer is almost negligible. Specifically, under both approximations the dipole mode (D) is red-shifted from the value  $\omega_M$  and a hybridized quadrupole mode (Q) appears at almost identical normalized frequencies. In contrast, the atomistic description shows a different behavior. While the normalized frequency of the dipole mode is the same for  $d = 0.5$  nm,

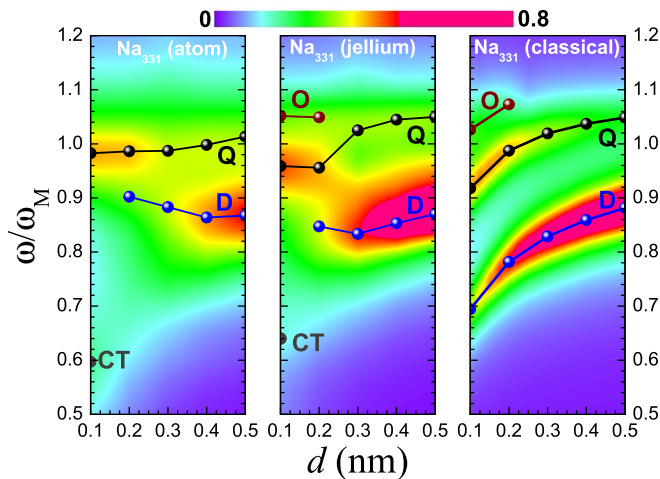


FIG. 2: (Color online) Contour plots of the normalized absorption cross section  $[\sigma_{\text{abs}}(\omega)/(2\pi R^2)]$  of a  $\text{Na}_{331}$  dimer vs the distance  $d$  as defined in the text. From left to right: atom/TDDFT, jellium/TDDFT, classical local optics. The frequencies of the different LSP modes (D: coupled dipole, Q: hybridized quadrupole, O: hybridized octupole, CT: charge transfer) are obtained from the local maxima of the absorption spectrum at each distance.

discrepancies already show up at  $d = 0.4$  nm. Moreover, the normalized frequency of the mode Q is slightly smaller. This can be attributed to the fact that the atomic cluster is not entirely spherical, affecting the hybridization process which is mediated by the EM near-field.

As is well-known, the classical description is not valid in the charge-transfer regime. [fig. 2](#) demonstrates that this regime is reached for  $d \simeq 0.3$  nm for the jellium model. In this case, the frequency of the D mode stabilizes and the spectral weight of the mode decreases as the nanoparticles get closer. Consequently the hybridized Q mode becomes dominant for  $d = 0.2$  nm. Furthermore, a weak hybridized octupole mode O appears. At a distance of  $d = 0.1$  nm, the mode D is completely quenched, and a very weak signature of a charge transfer mode (CT) appears instead [20]. However, the details of the atomic structure in the gap region between the nanoparticles are crucial when determining the intensity of the charge transfer current. In fact, charge transfer effects are already visible for a distance of  $d = 0.4$  nm. In turn, the CT mode in the almost-touching limit ( $d = 0.1$  nm) can be clearly discriminated in the absorption spectrum.

The importance of the atomic structure at sub-nanometric distances is further illustrated in [fig. 3](#), where we show the electric potential  $\delta\Phi$  along the dimer axis under driving by an external monochromatic field of amplitude  $E_0$  in resonance with the D mode ( $d = 0.3$  nm).  $\delta\Phi$  can be easily obtained by solving the Poisson equation corresponding to the charge density  $-e\delta n(\mathbf{r}, \omega)$  given in [Eq. 1](#). The jellium model clearly overestimates  $\delta\Phi$ , reflecting its well known inadequacy for quantitative predictions

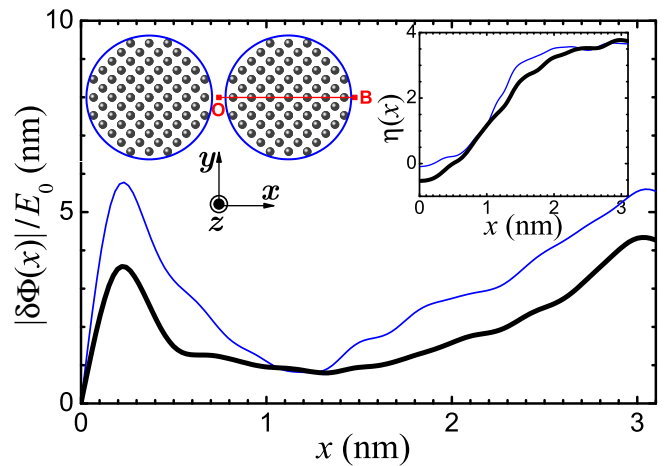


FIG. 3: (Color online) Amplitude  $|\delta\Phi(x)|$  of the induced electric potential along the OB segment (see upper left inset) of a  $\text{Na}_{331}$  dimer corresponding to the coupled dipole mode D ( $d = 0.3$  nm). Thick line: atom/TDDFT, thin line: jellium/TDDFT. The phase difference  $\eta(x)$  between the external and the induced fields is depicted in the upper right inset.

in nano-electronics [50]. However, it is interesting to note that the atomic structure does not strongly affect the phase of the electric potential (see right inset of [fig. 3](#)).

As commented above, a nanoparticle dimer has been considered as a prototypical system to test light harvesting properties of nanoplasmonic devices. Therefore, it is worth analyzing how the atomistic description affects both the modal shape and electric field enhancement (EFE) associated with the different resonances of the cluster dimer. As we have shown in [fig. 2](#), for  $d > 0.3$  nm the optical response of the dimer is dominated by the dipolar mode. In the left panels of [fig. 4](#) we render the electric field amplitudes for this D mode calculated at  $d = 0.4$  nm for both atom/TDDFT (upper panel) and jellium/TDDFT (lower panel) approaches. Notice that the scale is normalized to the maximum value of the E-field amplitude in each case. As expected, the modal shape is very similar in the two cases although the D mode for the atom/TDDFT approach is a bit more delocalized than the jellium/TDDFT counterpart. This results in a smaller EFE at the center of the  $\text{Na}_{331}$  dimer: the EFE is reduced by a factor of 2 when the atomic structure is included in the calculation (see [fig. 5](#)). The influence of the atomic structure in both the modal shape and EFE is even more critical when analyzing the quadrupole mode Q at shorter distances (see central panels of [fig. 4](#)). For the two distances ( $d = 0.2$  and  $d = 0.1$  nm), the Q mode for the atom/TDDFT description is much more delocalized than that emerging from the jellium/TDDFT numerical calculation. Whereas in this last case the E-field is still strongly localized in the region between the two clusters, the E-field amplitude for the Q mode in the atomistic calculation is more uniformly distributed along the surfaces

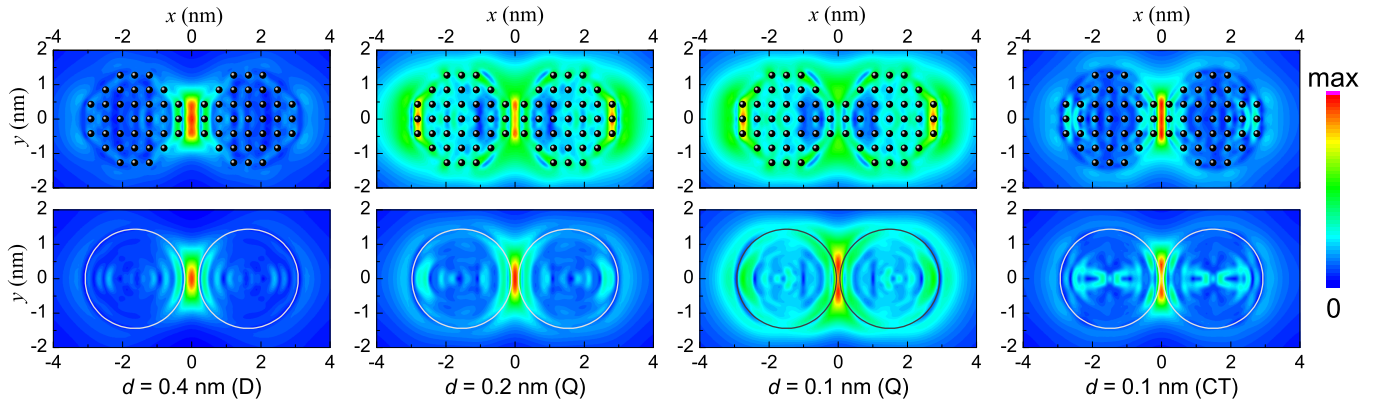


FIG. 4: (Color online) Contour plots of the electric field amplitude evaluated on the  $XY$  plane of the dimer at four selected resonances. Upper row: atom/TDDFT; lower row: jellium/TDDFT calculations. From left to right: dipolar mode D ( $d = 0.4$  nm); quadrupole mode Q ( $d = 0.2$  nm), Q mode ( $d = 0.1$  nm) and charge transfer CT mode ( $d = 0.1$  nm). Only the positions of the atoms lying in the  $XY$  plane are depicted. In each panel the E-field amplitude is normalized to its maximum value [c.f., fig. 5].

of the two clusters. Remarkably, for  $d = 0.1$  nm, the maximum EFE does not appear at the region between the nanoparticles as in the jellium/TDDFT description, but at the opposite ends of the two clusters. This delocalization of the EM-field modal shape provokes a strong reduction of the EFE for these two distances when comparing the atom/TDDFT approach with the jellium/TDDFT calculation, as shown in fig. 5. The right panels of fig. 4 show the modal shape of the CT mode for the two TDDFT calculations. It is interesting to note that the CT mode is much less sensitive to the atomic structure than the Q mode.

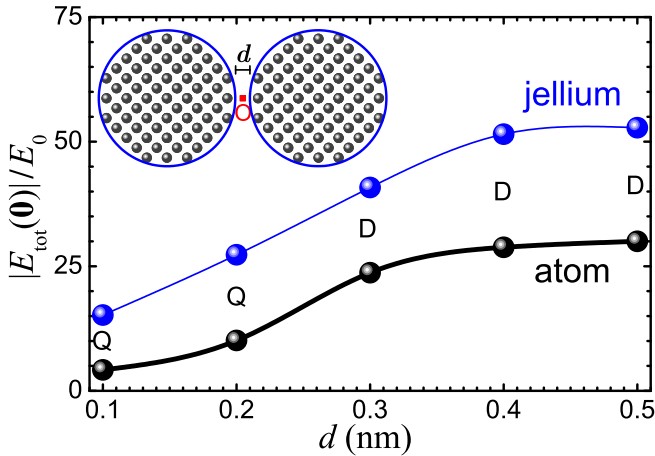


FIG. 5: (Color online) Electric field enhancement at the center  $O$  of the  $\text{Na}_{331}$  dimer corresponding to the dominant resonance of the absorption spectrum, as indicated in the figure itself. The connecting lines are guides to the eye.

By using *ab-initio* TDDFT calculations for analyzing the optical response of metal nanoparticle dimers, we have been able to demonstrate that the atomic structure of the

metal clusters plays a key role for determining accurately both the absorption cross section and electric field enhancement associated with these nanoplasmonic devices. This effect is more critical when the distance between the nanoparticles is smaller than around 0.3 nm. From a quantitative perspective, the inclusion of the ionic structure into the TDDFT calculations has a similar influence as the incorporation of both the electron density spill-out and non-locality in jellium-based TDDFT calculations when comparing them to the classical EM approaches. In conclusion, atoms matter in nanoplasmonics and it is mandatory to go beyond the usual jellium approach in TDDFT calculations if a quantitative description of quantum effects in nanoplasmonic structures is required.

This work has been funded by the European Research Council (ERC-2011-AdG Proposal No. 290981). We also acknowledge financial support from the European Research Council (ERC-2010-AdG Proposal No. 267374), Spanish Grants (MAT2011-28581-C02-01 and FIS2010-21282-C02), Grupos Consolidados UPV/EHU (IT-578-13), COST actions: CM1204, MP1306, and EC project CRONOS (Grant number 280879-2). Useful discussions with Prof. J.C. Cuevas and A. Varas are also acknowledged.

\* Electronic address: [pablo.garciagonzalez@uam.es](mailto:pablo.garciagonzalez@uam.es)

† Electronic address: [fj.garcia@uam.es](mailto:fj.garcia@uam.es)

- [1] J. N. Anker, W. P. Hall, O. Lyandres, N. C. Shah, J. Zhao, and R. P. Van Duyne, *Nature Mater.* **7**, 442 (2008).
- [2] T. Vo-Dinh, A. Dhawan, S. J. Norton, G. K. Houry, H.-N. Wang, V. Misra, and M. Gerhold, *J. Phys. Chem. C* **114**, 7480 (2010).
- [3] M. A. Noginov, G. Zhu, A. M. Belgrave, R. Bakker, V. M. Shalaev, E. E. Narimanov, S. Stout, E. Herz, T. Suteewong,

- and U. Wiessner, *Nature* **460**, 1110 (2009).
- [4] R. F. Oulton, V. J. Sorger, T. Zentgraf, R. M. Ma, C. Gladsten, L. Dai, G. Bartal, and X. Zhang, *Nature* **461**, 629 (2009).
- [5] P. Berini and I. De Leon, *Nature Photon.* **6**, 16 (2011).
- [6] C. R. Ward, F. Hüser, F. Pauly, J. C. Cuevas, and D. Natelson, *Nature Nano.* **5**, 732 (2010).
- [7] M. Galperin and A. Nitzan, *Phys. Chem. Chem. Phys.* **14**, 9421 (2012).
- [8] J. A. Schuller, E. S. Barnard, W. Cai, Y. C. Jun, J. S. White, and M. L. Brongersma, *Nature Mat.* **9**, 193 (2010).
- [9] A. Aubry, A. I. Fernández-Domínguez, Y. Sonnefraud, S. A. Maier, and J. B. Pendry, *Nano Lett.* **10**, 2574 (2010).
- [10] P. Muhlschlegel, H. J. Eisler, O. J. F. Martin, B. Hecht, and D. W. Pohl, *Science* **308**, 1607 (2005).
- [11] L. Novotny and N. van Hulst, *Nature Phot.* **5**, 83 (2011).
- [12] N. J. Halas, S. Lal, W.-S. Chang, S. Link, and P. Nordlander, *Chem. Rev.* **111**, 3919 (2011).
- [13] R. Ruppín, *Opt. Comm.* **190**, 205 (2001).
- [14] J. M. McMahon, S. K. Gray, G. C. Schatz, *Phys. Rev. Lett.* **103**, 097403 (2009).
- [15] S. Raza, G. Toscano, A.-P. Jauho, M. Wubs, and N. A. Mortensen, *Phys. Rev. B* **84** 121412(R) (2011).
- [16] C. David, and F. J. García de Abajo, *J. Phys. Chem. C* **115**, 19470 (2011).
- [17] A. I. Fernandez-Dominguez, A. Wiener, F. J. Garcia-Vidal, S. A. Maier, and J. B. Pendry, *Phys. Rev. Lett.* **108**, 106802 (2012).
- [18] A. I. Fernandez-Dominguez, P. Zhang, Y. Luo, S. A. Maier, F. J. Garcia-Vidal, and J. B. Pendry, *Phys. Rev. B* **86**, 241110(R) (2012).
- [19] T. Christensen, W. Yan, S. Raza, A.-P. Jauho, N. A. Asger Mortensen, and M. Wubs *ACS Nano* (in press) (2014).
- [20] R. Esteban, A. G. Borisov, P. Nordlander, and J. Aizpurua, *Nature Commun.* **3**, 825 (2012).
- [21] X. Ma and R. Mittra, *App. Phys. Lett.* **101**, 233111 (2012).
- [22] Y. Luo, A. I. Fernández-Domínguez, A. Wiener, S. A. Maier, and J. B. Pendry, *Phys. Rev. Lett.* **111**, 093901 (2013).
- [23] J. Zuolaga, E. Prodan, P. Nordlander, *Nano Lett.* **9**, 887 (2009).
- [24] D. C. Marinica, A. K. Kazansky, P. Nordlander, J. Aizpurua, and A. G. Borisov, *Nano Lett.* **12** 1333 (2012).
- [25] L. Stella, P. Zhang, F. J. García-Vidal, A. Rubio, and P. García-González, *J. Phys. Chem. C* **117**, 8941 (2013).
- [26] K. Andersen, K. L. Jensen, N. A. Mortensen, and K. S. Thygesen, *Phys. Rev. B* **87**, 235433 (2013).
- [27] T. V. Teperik, P. Nordlander, J. Aizpurua, and A. G. Borisov, *Opt. Express* **21**, 27306 (2013).
- [28] E. Runge, and E.K.U. Gross, *Phys. Rev. Lett.* **52**, 997 (1984).
- [29] M. A. L. Marques, N. T. Maitra, F. M. S. Nogueira, E. K. U. Gross, and A. Rubio (Eds.), *Fundamentals of Time-Dependent Density Functional Theory* (Springer, Berlin, 2012).
- [30] W. A. de Heer, *Rev. Mod. Phys.* **65**, 611 (1993).
- [31] M. Brack, *Rev. Mod. Phys.* **65**, 677 (1993).
- [32] G. Onida, L. Reining, and A. Rubio, *Rev. Mod. Phys.* **74**, 201 (2002).
- [33] S. M. Morton, D. W. Silverstein, and L. Jensen, *Chem. Rev.* **111** 3962 (2011).
- [34] P. Nordlander, C. Oubre, E. Prodan, K. Li, and M. I. Stockman, *Nano Lett.* **4**, 899 (2004).
- [35] I. Romero, J. Aizpurua, G. W. Bryant, F. J. Garcia de Abajo, *Opt. Express* **14**, 9988 (2006).
- [36] K. J. Savage, M. M. Hawkeye, R. Esteban, A. G. Borisov, J. Aizpurua, and J. J. Baumberg, *Nature* **491**, 574 (2012).
- [37] J. A. Scholl, A. Garcia-Etxarri, A. L. Koh, and J. A. Dionne, *Nano Lett.* **13**, 564 (2013).
- [38] M. S. Tame, K. R. McEnery, S. K. Özdemir, J. Lee, S. A. Maier, and M. S. Kim, *Nature Physics* **9**, 329 (2013).
- [39] T. V. Teperik, P. Nordlander, J. Aizpurua, and A.G. Borisov, *Phys. Rev. Lett.* **110**, 263901 (2013).
- [40] N. Troullier and J. L. Martins, *Phys. Rev. B* **43**, 1993 (1991).
- [41] A detailed account of the relaxation effects will be discussed elsewhere (A. Varas *et al*, in preparation).
- [42] A. Rubio, J. A. Alonso, X. Blase, L. C. Balbas, and S. G. Louie, *Phys. Rev. Lett.* **77**, 247 (1996).
- [43] I. Vasiliev, S. Ogut, and J. R. Chelikowsky, *Phys. Rev. Lett.* **82**, 1919 (1999).
- [44] J.-O. Joswig, L. O. Tunturivuori, and R. M. Nieminen, *J. Chem. Phys.* **128**, 014707 (2008).
- [45] K. Yabana and G. F. Bertsch, *Phys. Rev. B* **54**, 4484 (1996).
- [46] M. A. L. Marques, A. Castro, G. F. Bertsch, and A. Rubio, *Comput. Phys. Commun.* **151**, 60 (2003).
- [47] A. Castro, H. Appel, M. Oliveira, C. A. Rozzi, X. Andrade, F. Lorenzen, M. A. L. Marques, E. Gross, and A. Rubio, *Phys. Status Solidi B* **243**, 2465 (2006).
- [48] J.-H. Li, M. Hayashi, G.-Y. Guo, *Phys. Rev. B* **88**, 155437 (2013).
- [49] C. Yannouleas, E. Vigezzi, and R. A. Broglia, *Phys. Rev. B* **47**, 9849 (1993).
- [50] *Introducing Molecular Electronics*, edited by G. Cuniberti *et al.* (Springer, New York, 2005)